THE JOURNAL OF BIOLOGICAL CHEMISTRY VOL. 281, NO. 45, pp. 34421–34429, November 10, 2006

Functional and Biochemical Analysis of the N-terminal Domain of Phytochrome A*[S]

Received for publication, April 12, 2006, and in revised form, September 8, 2006 Published, JBC Papers in Press, September 11, 2006, DOI 10.1074/jbc.M603538200

Julieta L. Mateos[‡§1], Juan Pablo Luppi[§], Ouliana B. Ogorodnikova[¶], Vitaly A. Sineshchekov[¶], Marcelo J. Yanovsky[§], Silvia E. Braslavsky[‡], Wolfgang Gärtner[‡], and Jorge J. Casal[§2]

From the [‡]Max-Planck-Institut für Bioanorganische Chemie, Postfach 101356, D-45413 Mülheim an der Ruhr, Germany, [§]IFEVA, Facultad de Agronomía, Universidad de Buenos Aires, Avenue San Martín 4453,1417 Buenos Aires, Argentina, and [¶]Biology Department, M. V. Lomonosov Moscow State University, Moscow 119992, Russia

Phytochrome A (phyA) is a versatile plant photoreceptor that mediates responses to brief light exposures (very low fluence responses, VLFR) as well as to prolonged irradiation (high irradiance responses, HIR). We identified the *phyA-303* mutant allele of *Arabidopsis thaliana* bearing an R384K substitution in the GAF subdomain of the N-terminal half of phyA. *phyA-303* showed reduced phyA spectral activity, almost normal VLFR, and severely impaired HIR. Recombinant N-terminal half oat of PHYA bearing the *phyA-303* mutation showed poor incorporation of chromophore *in vitro*, despite the predicted relatively long distance (>13 Å) between the mutation and the closest ring of the chromophore. Fusion proteins bearing the N-terminal domain of oat phyA, β-glucuronidase, green fluorescent protein, and a nuclear localization signal showed physiological activity in darkness and mediated VLFR but not HIR. At equal protein levels, the *phyA-303* mutation caused slightly less activity than the fusions containing the wild-type sequence. Taken together, these studies highlight the role of the N-terminal domain of phyA in signaling and of distant residues of the GAF subdomain in the regulation of phytochrome bilin-lyase activity.

Plant photoreceptors monitor the cues provided by the light environment and trigger modifications that adjust growth and development to the prevailing conditions (1, 2). Phytochromes are sensors of red and far-red (FR)[3] light that bind an open chain tetrapyrrole chromophore (3, 4). *Arabidopsis thaliana* bears five phytochrome apoprotein genes (*PHYA* through *PHYE*) (5).

phyA is a versatile photoreceptor that induces seed germination in response to brief exposures to light (6, 7), which the seeds may experience during soil labor. phyA is also required to perceive the prolonged exposures to FR that the seedlings experience when they emerge from the soil under dense plant canopies (8). These two photoresponses mediated by phyA are of the types called very low fluence responses (VLFR) and high irradiance responses (HIR), respectively (9). Some physiological processes (*e.g.* inhibition of hypocotyl growth, unfolding of the cotyledons) exhibit both VLFR and HIR as two discrete phases of response, where VLFR saturates with infrequent FR pulses and HIR requires very frequent or continuous FR (10). HIR requires *cis*-acting elements at target gene promoters (11) and domains of the phyA molecule itself (12) that are dispensable for VLFR.

The N-terminal domain of phytochromes bears the chromophore attachment site (13) and provides differential spectral selectivity to phyA (more active under FR than red light) compared with phyB (more active under red light than FR) (14). The C-terminal domain contains a histidine kinase-related sequence motif that is able to mediate phosphorylation (15, 16), two PAS (domain named after Per, Arnt, and Sim) motifs important for downstream signaling in the context of the full molecule (17), and residues necessary for dimerization (18, 19) and targeting to the nucleus upon light activation (20, 21). Two recent findings have focused attention on the N-terminal domain of phytochromes. First, the N-terminal domain of phyB fused to green fluorescent protein (GFP), β-glucuronidase (GUS), and a nuclear localization signal (NLS) is physiologically active (21, 22). This result contradicts the previous extended consensus that the C-terminal domain of phytochromes was responsible for downstream signaling. Second, Wagner *et al.* (23) have determined the crystal structure of the conserved N terminus photosensory core of a bacteriophytochrome from *Deinococcus radiodurans* (*Dr*BphP).

The results presented here provide insight into the physio-

* This work was supported in part by Deutsche Forschungs Gemeinschaft (DFG) Grant BR 901/14-1,/14-2 (to S. E. B.), Russian Foundation for Basic Research Grant 05-04-49549 (to V. A. S.), and University of Buenos Aires (G021) and Agencia Nacional de Promoción Científica y Tecnológica (PICT 11631) grants (to J. J. C.). The costs of publication of this article were defrayed in part by the payment of page charges. This article must therefore be hereby marked "*advertisement*" in accordance with 18 U.S.C. Section 1734 solely to indicate this fact.

[S] The on-line version of this article (available at http://www.jbc.org) contains supplemental Table S1.

[1] Supported by fellowships from National Research Council of Argentina and DFG.

[2] To whom correspondence should be addressed. Tel.: 5411-4524-8070; Fax: 5411-4514-8730; E-mail: casal@ifeva.edu.ar.

[3] The abbreviations used are: FR, far-red light; *Dr*BphP, bacteriophytochrome from *D. radiodurans*; GAF, domain named after cyclic GMP, Adenylyl cyclase and FhlA; GFP, green fluorescent protein; GUS, β-glucuronidase; HIR, high irradiance response; lumi-R, red-shifted transient produced upon excitation of P_r; MALDI-TOF, matrix-assisted laser desorption ionization time-of-flight; NLS, nuclear localization signal; PCB, phycocyanobilin; P_r, P_{fr}, red and far-red light-absorbing forms of phytochrome; phyA, phyB, holoprotein of phytochromes A and B, respectively; PHYA, PHYB, apoprotein of phytochromes A and B, respectively; *PHYA*, phytochrome A encoding gene; phyA-65-WT, 65-kDa N terminus domain of wild-type oat phytochrome; phyA-65-R384K, 65-kDa N terminus domain of oat phytochrome with arginine 384 mutated for lysine; VLFR, very low fluence response; WT, wild type.

Supplemental Material can be found at: http://www.jbc.org/cgi/content/full/M603538200/DC1

logical function and biochemical activity of the N-terminal domain of phyA. By using a forward genetics approach we have identified a mutation of the *PHYA* gene that impairs chromophore binding despite its relative distant position to the attachment site within the GAF domain. We also report on the biological activity of an N-terminal domain fragment of phyA and the impact of the aforementioned mutation on this activity.

EXPERIMENTAL PROCEDURES

Mutant Screening—Ethylmethane sulfonate mutagenized seeds of *A. thaliana* (accession Landsberg *erecta*; Lehle Seeds, Round Rock, TX) were sown in clear plastic boxes (175 × 225 mm^2 × 45 mm in height) containing 0.8% agar, incubated 3 days in darkness at 7 °C, and then transferred to continuous FR for 4 days (12).

Cloning and Sequencing of the phyA-303 Allele—Total mRNA was obtained with RNA Easy Plant kit (Qiagen) and used as a template for reverse transcription PCR to produce *PHYA* cDNA (primers are described in supplemental Table S1). The fragment was cloned into pUC19 vector and sequenced at Automatic DNA Isolation and Sequencing (Max-Planck-Institut für Züchtungsforschung).

Physiological Characterization—The wild-type (WT) strain and the *phyA-201* (24), *phyA-205* (25), *hy1* and *hy2* mutants (26–28) are all in the Landsberg *erecta* background. Fifteen seeds of each genotype were sown in clear plastic boxes and exposed to the different light treatments as described (12). Interference filters were used to provide light at 700, 710, 720 nm (CVI Laser Corp.), or 743 nm (Mainz Schott).

Hypocotyl length was measured with a ruler, and the angle between the cotyledons was measured with a protractor. Data corresponding to the 10 tallest seedlings from each box were averaged (one replicate) (12).

In the experiments involving chromophore feeding, 3 μl of biliverdin IXα solution of the indicated concentrations were added to each seed under green light immediately after the red light exposure used to induce germination. The boxes were kept in darkness at 23 °C for 20 h and then placed in darkness or under the various light treatments for 3 days before measurements.

Low Temperature in Vivo Phytochrome Fluorescence—Fluorescence emission spectra at low temperature (85 K) were recorded in the hypocotyl plus root of 4-day-old seedlings grown in darkness with a laboratory-designed spectrofluorometer based on two double grating monochromators as described (12).

PHYA Protein Blots—Aliquots of plant extracts (29) containing ~20 μg of crude protein were separated on SDS-polyacrylamide gels and blotted to polyvinylidene difluoride membranes (Millipore) for 1 h at ~200 mA. Immunodetection of *Arabidopsis* PHYA was performed using monoclonal antibody 073D (kindly provided by Richard Vierstra, University of Wisconsin). Detection of recombinant proteins and oat PHYA-65-GFP-GUS-NLS fusion proteins from transgenic plants was performed using monoclonal antibody Oat25 (kindly provided by Lee Pratt, University of Georgia). In all cases the blot was incubated overnight at 4 °C with the corresponding primary antibody. After washing, the membrane was incubated with 1:1000 dilution of horseradish peroxidase-conjugated antibody to mouse IgG (Sigma) for 1–2 h at room temperature. Bands were visualized by the chemoluminescent method. Band intensity was quantified with the Scion Image Software.

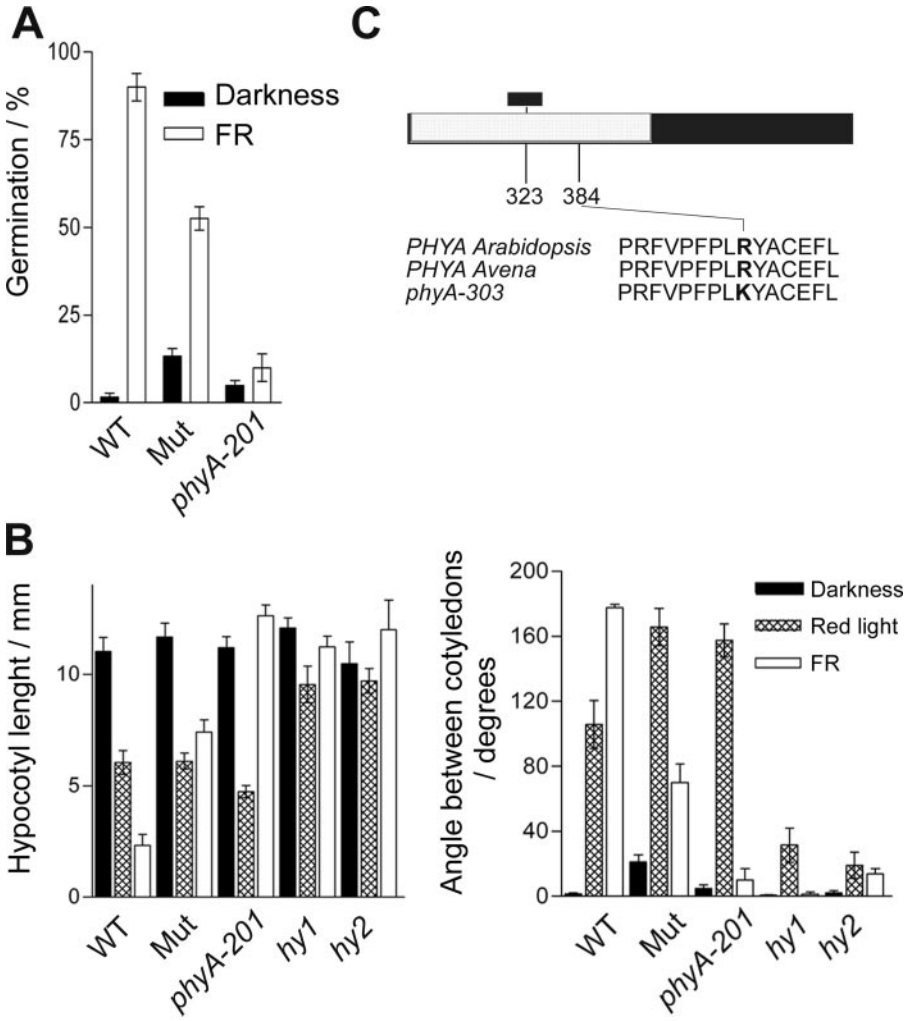

FIGURE 1. **Identification of a novel *phyA* mutant allele.** *A*, the mutant (*Mut*) shows partial induction of seed germination by FR. *B*, mutant seedlings show severely impaired hypocotyl growth inhibition and cotyledon unfolding responses of the seedling to FR and normal responses to red light (30 μeinstein $m^{-2} s^{-1}$). *C*, sequencing the *PHYA* gene identified an R384K substitution. The mutant was named *phyA-303*. Physiological data are means and S.E. of three to six replicate boxes.

Heterologous Expression of PHYA Gene, Mutagenesis, and Protein Purification—For yeast expression the N-terminal domain of oat *PHYA* (nucleotides 1–1795, which corresponds to residues 1–595) was cloned into a derivative from the pHILD2 vector (Invitrogen), placing a His_6 tail at the C-terminal end of the sequence. The R384K mutation was introduced by site-directed mutagenesis with the QuikChange Stratagene kit. The presence of the mutation was confirmed by sequencing. Plasmids were introduced into *Pichia pastoris GS115*, and expression was carried out according to the manufacturer's instructions (Pichia expression kit; Invitrogen). For expression in bacterial host, the N-terminal cDNA from oat *PHYA* was cloned into pMEX8 vector. The mutation was produced as in the yeast system. Generation of the reverted gene was achieved by site-directed mutagenesis. Expression was accomplished in *Escherichia coli* Top10F′ strain (1-liter culture). For yeast and bacteria, cells were disrupted at liquid N_2 temperature using an Ultra-Turrax, and the protein solution was clarified by ultracentrifugation at 14,000 rpm, 4 °C. The supernatant was used directly for chromophore assembly experiments. Detection of apoprotein was also checked in protein blots. His-tagged proteins were purified over the BD TALON™ metal affinity resin (Clontech Laboratories, Inc., Palo Alto, CA). Elution was carried out using imidazol, and buffer changes were performed by either dialysis with 10 K dialysis frames (Slide-A-Lyzer; Pierce) or by gel filtration using the PD-10 columns (Amersham Biosciences). All the primers are described in supplemental Table S1.

Measurements of Δ *Absorbance*—Δ absorbance spectra after red/far-red irradiations were obtained as described earlier (30). ΔΔ absorbance was calculated as the difference between Δ absorbance at 654 and 715 nm (assembly experiments) or 660 and 730 nm (seedling extracts). Seedling extracts were obtained as described (31).

Chromophore Preparation—Phycocyanobilin (PCB) was extracted from *Spirulina platensis* as described (32). Biliverdin IXα was derived from bilirubin by oxidation (33) and was purified by high pressure liquid chromatography with the column Inertsil-3-C_{18} 7,6 × 250 mm and solvent EtOH:MeOH:Acetone:H_2O (20:20:20:40). Fractions were lyophilized and stored at −70 °C in darkness.

Plasmid Construction and Plant Transformation—Construction of the *PHYA-65-WT-GFP-GUS-NLS* chimeric gene was performed in several steps fusing all the four genes. The nuclear localization signal from SV40 was obtained by annealing of oligonucleotides (supplemental Table S1). The fragment encoding the N-terminal domain of *PHYA* from oat was amplified by PCR and fused to the sequences encoding the GFP-GUS-NLS fragment. The chimeric gene was generated in pBSKSII and subcloned into pCHF3 vector under the 35S promoter. To generate the PHYA-65-R384K-GFP-GUS-NLS fusion, the fragment of the WT *PHYA* cDNA was replaced by the oat-mutated version. *A. thaliana phyA-201* was transformed as described (34). Transformed plants were selected against 50 μg/ml kanamycin, and T2 seeds were tested for a 3:1 segregation of kanamycin resistance. T3 seeds of positive T2 lines were tested for homozygous genetic segregation and used for further experiments.

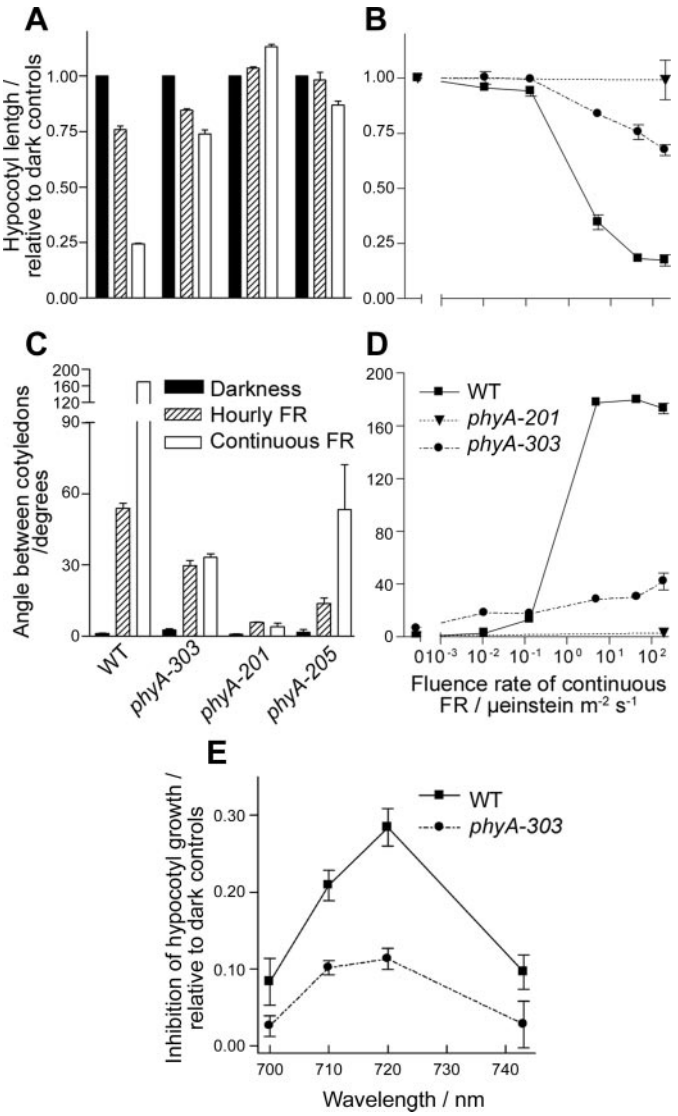

FIGURE 2. **Physiological characterization of the *phyA-303* mutant.** Hypocotyl length relative to dark controls (*A*, *B*) and angle between the cotyledons (*C*, *D*), in response to FR given either continuously (10 μeinstein m^{-2} s^{-1}) or as hourly pulses (3 min, 200 μeinstein m^{-2} s^{-1} to achieve equal hourly fluence rate in both cases: 36,000 μeinstein m^{-2} h^{-1}) (*A*, *C*) and in response to different fluence rates of continuous FR (*B*, *D*). Seedlings were also grown under continuous irradiation with selected wavelengths (1 μeinstein m^{-2} s^{-1}), and the phyA-mediated inhibition of hypocotyl growth was calculated for each wavelength as the difference between the length of WT or *phyA-303* and the length of *phyA-201* (null allele) after normalization to hypocotyl length in darkness (*E*). Results similar to those reported in *panels A* and *B* were obtained if continuous and hourly FR were provided at equal fluence rate (10 μeinstein m^{-2} s^{-1}). The *phyA-201* and *phyA-205* mutants are included for comparative purposes. Data are means and S.E. of ten or three (*E*) replicate boxes.

Confocal Microscopy—Transgenic seedlings were grown on agar (0.8% w/v) plates for 3 days in the dark. Etiolated seedlings were kept in the dark or exposed to either white light or FR. All subsequent manipulations were performed under green safelight. To visualize nuclei and cell walls, seedlings were stained with 0.1 μM aqueous solution of propidium iodide for 5–10 min (21). Fluorescence of GFP and propidium iodide was visualized by a confocal laser-scanning microscope (Zeiss LSM5, Pascal) with standard fluorescein isothiocyanate (GFP) and tetramethylrhodamine isothiocyanate filters (propidium iodide). Images

corresponding to dark were taken within the first minute of microscope observation. Similar results were obtained with hypocotyl and root samples. At least 10 seedlings were analyzed for each genotype, and representative images were processed using Adobe Photoshop 8.0 software.

RESULTS

Novel phyA Mutant Allele—To obtain mutants impaired in the HIR but retaining a significant VLFR we used mutagenized seeds of *A. thaliana* and selected seedlings with long hypocotyl and poorly opened cotyledons under continuous FR (typical of poor HIR) produced by seeds that germinated under FR (typical of normal VLFR) (12). The mutant that we describe here was confirmed in the next generation by its ability to germinate under FR and its impaired hypocotyl growth and cotyledon angle responses under FR (Fig. 1*A*). No differences between the WT and the mutant were observed in darkness or under red light (Fig. 1*B*). The latter excluded mutations at loci involved in the synthesis of the chromophore, which are predicted to affect all phytochromes and therefore not only the response to FR but also to red light (see chromophore synthesis mutants *hy1* and *hy2* in Fig. 1*B*) (27, 28, 35). The null *phyA-201* mutant failed to complement the mutant selected here (*e.g.* cotyledon angle under FR was $<10°$ for the F1 generation of their cross), suggesting that the *PHYA* gene itself was affected. The *PHYA* gene was cloned and sequenced completely from two independent plants. A single base pair change (G-1337 to A) was observed, which resulted in the R384K substitution (Fig. 1*C*). The mutation falls in the GAF domain of PHYA, 61 amino acid residues away from the chromophore-bearing cysteine residue. The allele obtained here had not been reported earlier and was named *phyA-303*.

Physiological Characterization—For inhibition of hypocotyl growth and promotion of cotyledon unfolding, the VLFR saturates with infrequent FR pulses (*e.g.* one pulse every hour), whereas HIR requires very frequent or continuous excitation with FR (10). In the *phyA-303* mutant, the VLFR (difference between hourly FR and darkness) of hypocotyl growth and cotyledon unfolding was close to the WT levels, but the HIR (difference between the effects of continuous and hourly FR) was severely impaired (Fig. 2, *A* and *C*). Another distinctive feature of the HIR is its strong fluence rate dependence (9). The *phyA-303* mutant showed very weak fluence rate dependence (Fig. 2, *B* and *D*) but normal wavelength dependence of the phyA-mediated response (Fig. 2*E*).

Spectral Activity and Protein Abundance of phyA in phyA-303—Low temperature phytochrome fluorescence was severely reduced in dark-grown seedlings of *phyA-303.* Subtraction of the residual fluorescence signal observed in a null allele of phyA (*i.e.* the signal accounted for mainly by phyB) indicates that the phyA signal in the mutant is less than 0.2 of the WT signal (Fig. 3*A*). This result is consistent with the ΔΔ absorbance signal observed in seedling extracts (WT, 0.0048; *phyA-303*, 0.0019; null mutant *phyA-201*, 0.0010; *i.e.* the *phyA-303* mutant retains 0.2 of the WT signal). The residual phytochrome photochemical activity in the mutant was qualitatively similar to that observed in the WT in terms of P_r-lumi-R photoequilibrium (Fig. 3*B*) and fluorescence spectrum (Fig. 3*C*). Immunochemically detected levels of PHYA were also reduced in the *phyA-303*, but this effect appears not as intense as the reduction in spectral activity (Fig. 3*D*).

Because the phenotype of the *phyA-303* mutant is observed under FR and not in darkness, we investigated whether the differences in PHYA protein levels were larger under FR due to increased instability of the mutated protein. Seedlings were

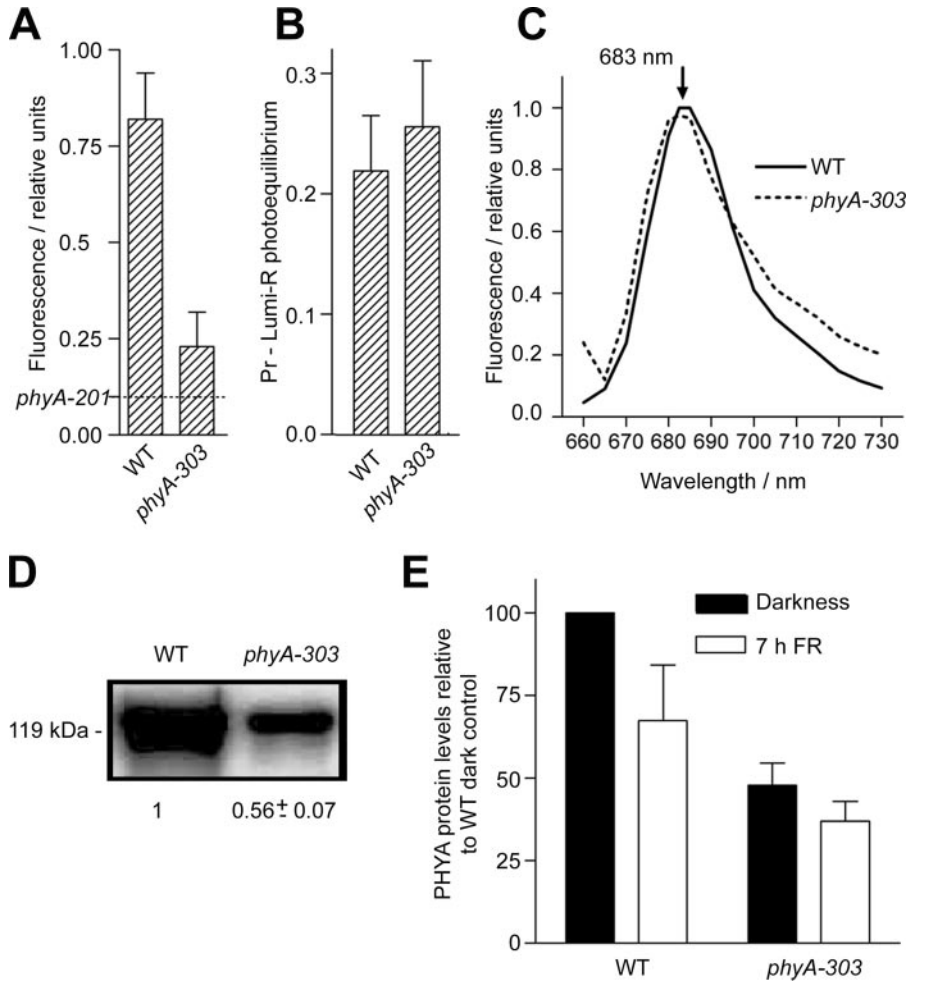

FIGURE 3. Dark-grown seedlings of the *phyA-303* mutant show reduced low temperature phytochrome fluorescence (*A*), normal P_r-lumi-R photoequilibrium (*B*), normal low temperature fluorescence spectrum (*C*), and reduced immunochemically detectable PHYA protein levels (expressed relative to the WT) (*D*). The effect of the *phyA-303* mutation on PHYA abundance is similar in darkness or under FR *E*, Data are means and S.E. of eight (*A*) or three (*D*, *E*) independent biological replicates.

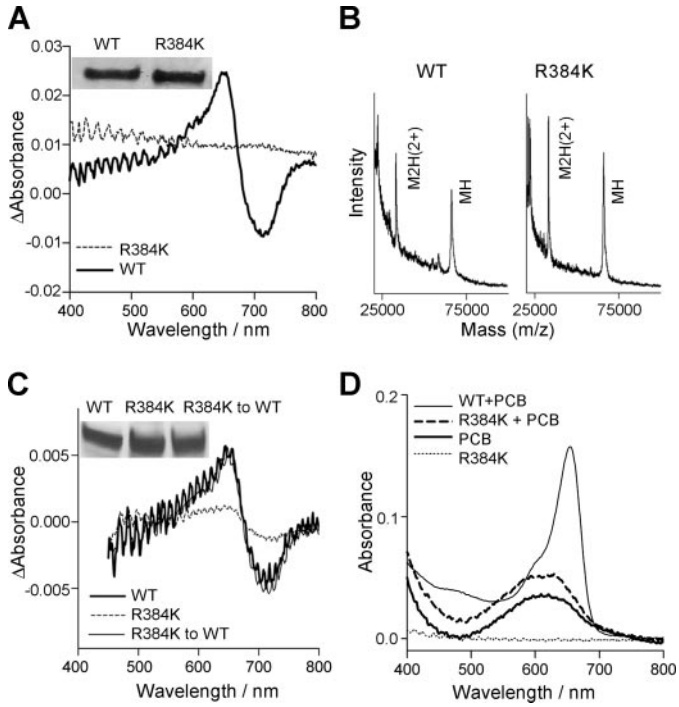

FIGURE 4. **Recombinant oat PHYA bearing an R384K substitution fails to incorporate chromophore *in vitro*.** *A*, spectrum of the absorbance difference between red- and FR-irradiated samples of PHYA-65-WT and PHYA-65-R384K obtained in yeast and assembled with PCB after purification. *B*, MALDI-TOF mass spectra in DHB matrix of PHYA-65-WT and PHYA-65-R384K obtained in yeast. *C*, spectrum of the absorbance difference between red- and FR-irradiated samples of PHYA-65-WT, PHYA-65-R384K, and PHYA-65-R384K to K384R obtained in *E. coli*. *D*, absorption spectrum of PHYA-65-WT and PHYA-65-R384K with or without PCB and PCB alone. *Insets*, immunoblots with Oat25 antibody to demonstrate equal amounts of protein used in the assay.

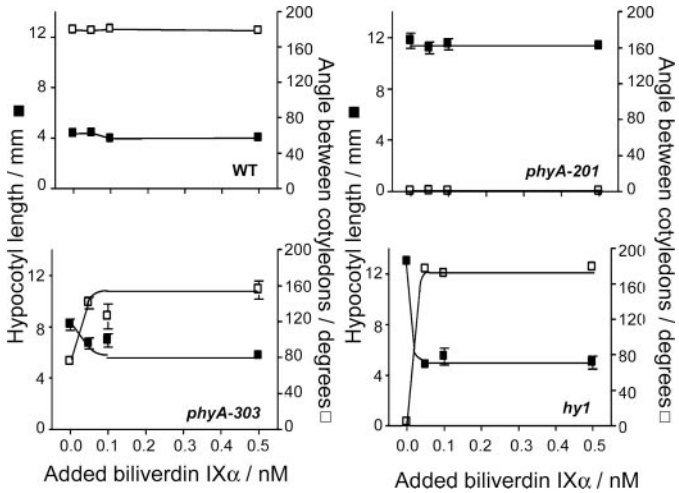

FIGURE 5. **Addition of biliverdin IXα to the growth medium partially restores the *phyA-303* phenotype under continuous FR (60 μeinstein m^{-2} s^{-1}).** Data are means and S.E. of three replicate boxes.

grown for 3 days in darkness and then exposed to continuous FR for 7 h. Exposure of WT seedlings to FR caused a small but detectable decrease in protein levels (10). The response of the *phyA-303* mutant was not proportionally larger than that observed in the WT (Fig. 3*E*).

Mutation R384K Impairs Chromophore Incorporation—The *phyA-303* mutant showed a stronger reduction in low temperature fluorescence signal than in protein levels (Fig. 3). Because P_r-lumi-R photoequilibrium of the residual phytochrome was normal (Fig. 3*B*), one might propose that the mutation could reduce the efficiency of chromophore incorporation. To test this hypothesis *in vitro* we expressed WT and R384K mutated *PHYA* gene of *Avena sativa*, which for practical reasons is normally used for *in vitro* studies (16, 36–38), in two heterologous systems (*E. coli or P. pastoris*). We expressed the first 595 amino acids of oat PHYA (PHYA-65) because the spectroscopical features of this domain are almost identical to those of full-length phytochrome and the truncated protein is expressed in higher yields and shows an improved stability (39).

When incubated with PCB, PHYA-65-WT yielded typical spectrophotometric features with maximum absorbance differences at 654 and 713 nm between samples irradiated with red or FR (Fig. 4, *A* and *C*). After incubation of an equal amount of the mutated PHYA-65-R384K with PCB, the Δ absorbance signal was weak (Fig. 4, *A* and *C*) and did not increase even after overnight incubation (data not shown), thus precluding kinetics analyses (40). The presence and integrity of the WT and mutant PHYA were confirmed by MALDI-TOF mass spectrometry of the purified recombinant proteins (Fig. 4*B*). Although weak, the residual signal showed normal parameters (Fig. 4*C*). As a control experiment, WT PHYA was reconstituted from PHYA-65-R384K by site-directed mutagenesis to regenerate arginine. The regenerated WT PHYA was identical to the originally recombinant WT PHYA in terms of spectral behavior (Fig. 4*C*) and kinetics of chromophore incorporation (data not shown).

The primary defect of PHYA-65-R384K is in chromophore incorporation rather than in phototransformation. The absorption spectrum of PHYA-65-R384K plus chromophore was similar to that of the chromophore alone (Fig. 4*D*), indicating that PHYA-65-R384K fails to normally incorporate the chromophore and change its environment and spectral properties. PHYA-65-WT incorporated the chromophore and showed a maximum shift to 654 nm compared with free chromophore.

Feeding with Biliverdin IXα Partially Rescues the phyA-303 Mutant—To investigate whether chromophore incorporation *in vivo* was limiting for the physiological output, we cultivated WT and *phyA-303* seedlings on agar supplemented with different doses of the chromophore precursor biliverdin IXα. The rationale behind this experiment was that if the inefficient incorporation of chromophore caused reduced responses to FR, increasing the amount of available chromophore might probably alleviate this defect. This expectation was met by the data (Fig. 5). In seedlings grown under continuous FR, addition of biliverdin IXα had no effects on the WT or the *phyA-201* (null allele) mutant but fully rescued the chromophore mutant *hy1* (35) and partially rescued the *phyA-303* mutant. The reduced protein levels observed in *phyA-303* (Fig. 3*D*) could account for the failure of biliverdin IXα to fully restore a WT response to continuous FR. Addition of biliverdin IXα had no effect in *phyA-303* seedlings grown under hourly pulses of FR (data not shown).

Physiological Output of Oat PHYA Amino-terminal Domain—The amino-terminal domain of PHYB is sufficient for signaling when fused to GFP, GUS, and NLS and expressed in a *phyB* null background (21, 22). Because our *in vitro* data had been

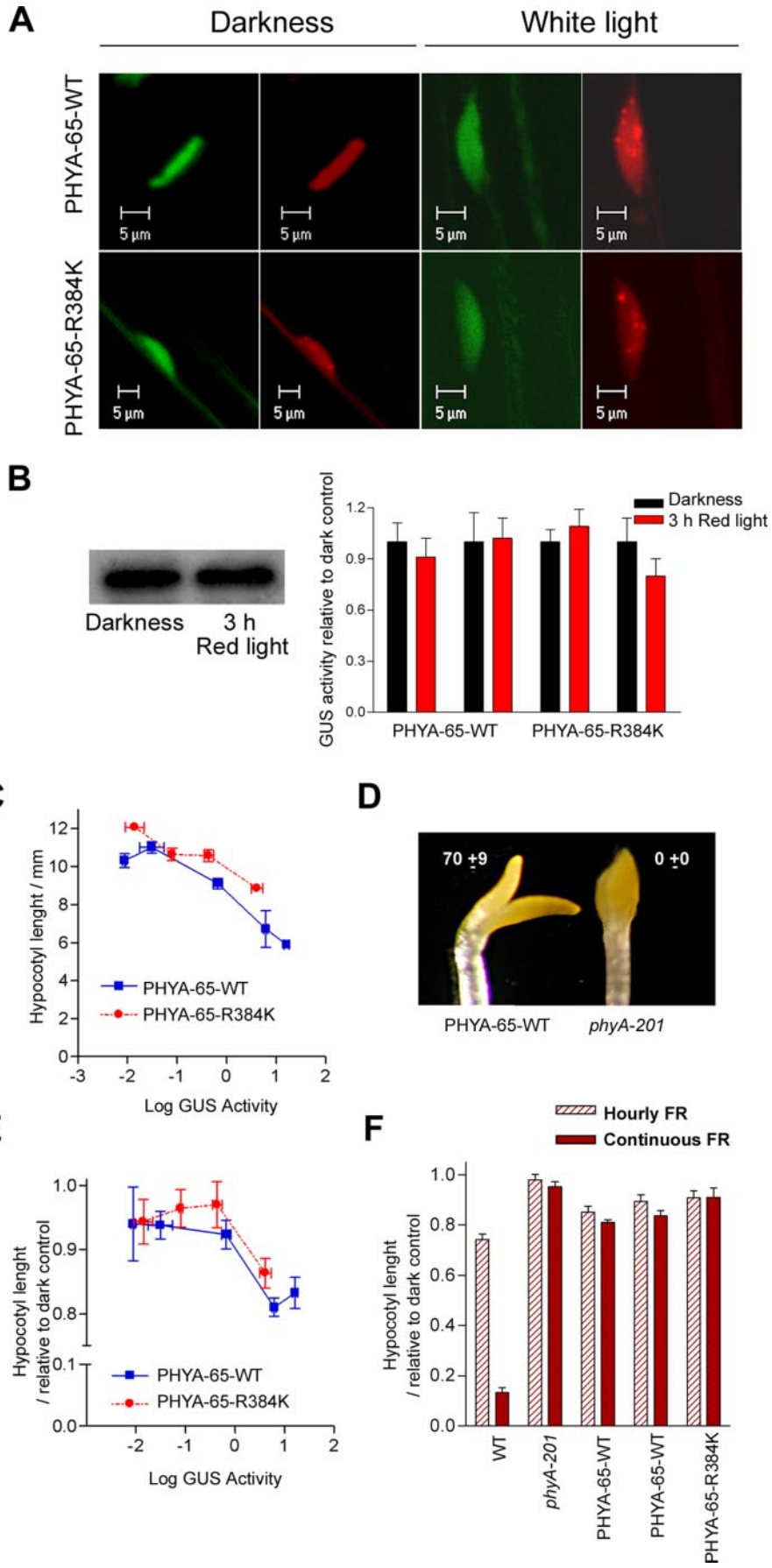

obtained with the amino-terminal domain of oat WT and mutated PHYA (amino acids 1–595), we decided to evaluate the *in vivo* performance of the oat PHYA N-terminal domain fused to GFP, GUS, and NLS in a *phyA*-null mutant background in *A. thaliana*. Previous studies demonstrating activity of the N terminus had been done with phyB (21, 22); thus, an additional interest of this experiment was to test whether the N terminus of phyA is also sufficient for downstream signaling.

We obtained five independent transgenic lines homozygous for the *PHYA* transgene fusion (PHYA-65-WT lines) and four lines for the *phyA-303* transgene fusion (PHYA-65-R384K lines). Taking advantage of the presence of GFP we investigated the cellular localization of the fusion proteins by confocal microscopy. Both PHYA-65-WT and PHYA-65-R384K showed nuclear expression in darkness and under illumination (Fig. 6*A*). The abundance of these fusion proteins measured by their GUS activity remained unaffected by the exposure of dark-grown seedlings to red light (Fig. 6*B*).

The physiological output of the different lines was plotted against their GUS activity driven by the fusion proteins. To our surprise, the length of the hypocotyl observed in independent transgenic lines grown in full darkness was inversely related to the GUS activity. This effect was somewhat larger for PHYA-65-WT than for PHYA-65-R384K (Fig. 6*C*). The two lines expressing the highest levels of GUS also showed unfolding of the cotyledons in darkness (Fig. 6*D*). The seedlings grown under continuous FR showed only a weak inhibition of hypocotyl growth by the light treatment, which reached a maximum of ~20% for the lines expressing the highest levels of GUS (Fig. 6*E*). Cotyledon unfolding retained dark control levels (*e.g.* mean ± S.E., cotyledon unfolding (in degrees) darkness, 70 ± 9; continuous FR, 65 ± 3). The PHYA-65-R384K lines had slightly less response than the PHYA-65-WT lines. Continuous and hourly pulses of FR were similarly effective to inhibit hypocotyl growth (Fig. 6*F*), indicating that the PHYA-65-WT or PHYA-65-R384K fusions were unable to produce a HIR.

The observed effect of PHYA-65-WT and PHYA-65-R384K on dark-grown seedlings could be accounted for by the action of the nuclear-localized protein fusions in their P_r form or by the P_{fr} form of these molecules established by a previous light exposure (*e.g.* the light pulse used to induce germination). To test the latter possibility, chilled seeds were incubated for 8 h under red light (22 °C) and subsequently transferred to darkness with or without a long wavelength FR pulse. This FR pulse, which is able to photo-convert most but not all P_{fr} to P_r, significantly reduced the phenotype of dark-grown seedlings expressing the protein fusion (*e.g.* PHYA-65-WT line, mean ± S.E., cotyledon unfolding (in degrees) without FR, 79 ± 11; with FR, 32 ± 7), indicating that the dark-grown seedling phenotype was at least partially due to the stable protein fusion (Fig. 6*B*) in the P_{fr} form.

DISCUSSION

The plant photoreceptor phyA mediates both VLFR and HIR. The *phyA-303* mutant allele and the N-terminal domain PHYA-65-GFP-GUS-NLS fusions produced here had differential ability to initiate VLFR and HIR. By using a genetic screening we have identified the *phyA-303* allele, bearing an R384K substitution. The HIR (*i.e.* the difference in response between hourly and continuous FR) is severely impaired in *phyA-303*, whereas the mutant phenotype is less evident under VLFR (pulsed) conditions (Fig. 2, *A* and *C*). This differential effect was not observed in the case of a *phyA-205* mutant, which carries a V631M mutation (25), retains normal levels of protein and photochemical activity (17), and is at least as affected in VLFR as in HIR (Fig. 2, *A* and *C*). The *phyA-303* mutant shows an ~50% reduction in PHYA protein levels and a more severe reduction in spectrally active phyA levels, but residual phyA has normal phototransformation parameters (Fig. 3) and physiological spectral activity (Fig. 2*D*) (41). Furthermore, recombinant protein bearing the *phyA-303* mutation showed poor bilin incorporation *in vitro* (Fig. 4) even after prolonged incubation. The physiological phenotype could therefore be accounted for, at least in principle, by a combination of less apoprotein and poor chromophore attachment. In accordance with the latter contention, addition of chromophore to the growth medium (predicted to alleviate its inefficient incorporation rate) partially restored the phenotype under continuous FR (Fig. 5) and had no effects under pulsed FR. Therefore, the HIR appears to require a higher threshold of photochemically active phyA than the minimum required for VLFR. Theoretically, this higher threshold could be involved in the formation of a HIR-specific complex with a signaling partner of phyA. The expression of PHYA-65-GFP-GUS-NLS fusions in a *phyA* null background restored a response to pulses of FR, which was not enhanced by continuous FR (Fig. 6, *E* and *F*).

The PHYA apoprotein catalyzes the formation of a thioether link with a bilin chromophore (42). The bilin lyase activity has been assigned to the GAF domain (amino acids 218–392 of *Arabidopsis* PHYA) (43). Little is known, however, about the specific role played by different residues in the dual function of this domain as substrate and catalytic regulator. Slow or poor *in vitro* chromophore incorporation has been reported for proteins mutated close to the cysteine

FIGURE 6. **Nuclear localization and physiological activity of PHYA-65-WT-GFP-GUS-NLS and PHYA-65-R384K-GFP-GUS-NLS fusion proteins expressed in *A. thaliana* seedlings of the *phyA-201* background.** *A*, fusion proteins are nuclear localized in darkness and upon exposure to light. Confocal images of hypocotyl cells from 4-day-old etiolated seedlings showing GFP or propidium iodide (*red*) fluorescence. *B*, fusion proteins are stable in the light. Immunoblots with Oat25 antibody against PHYA (*left*, signal only detectable for PHYA-65-WT) and GUS activity (*right*, two independent transgenic lines per construct) from seedlings grown in darkness for 3 days and either left in darkness or exposed to red light for 3 h before harvest. *C*, hypocotyl length in dark-grown seedlings is inversely related to the abundance of fusion proteins measured by the GUS activity of independent transgenic lines. Data are means and S.E. (whenever larger than the symbols) of ten boxes for hypocotyl length and six boxes for GUS activity. *D*, the PHYA-65-WT lines with highest GUS activity show partial cotyledon unfolding in darkness. Representative seedling and average data (and S.E. from ten replicate boxes) from one of the two PHYA-65-WT lines with highest GUS activity. Seedlings of the *phyA-201* mutant that do not express the fusion protein (*photograph*) or of the WT (not shown) exhibit no cotyledon unfolding in darkness. *E*, hourly pulses of FR (3 min, 200 μeinstein m^{-2} s^{-1}) cause hypocotyl growth inhibition. Hypocotyl length under pulsed FR is expressed relative to dark controls (shown in *panel C*). Data as in *panel C*. *F*, continuous FR (10 μeinstein m^{-2} s^{-1}) is not more effective than hourly FR. Data correspond to the three lines with highest GUS activity (see *panels C* and *E*).

323, between amino acids 309 and 326 (43–45). Based on the recently published crystal structure of the photosensory core of *Dr*BphP (23), the latter region involves residues in close contact with the chromophore.

The *phyA-303* mutation affects a residue conserved among plant and bacterial phytochromes but poorly conserved among the generic sequence of the GAF domains (43). *phyA-303* has a severe effect on chromophore incorporation despite the conservative nature of the Arg to Lys substitution in terms of amino acid charge and the lack of any impact on secondary structure. There are examples of substitutions that do not affect charge and yet have functional consequences. The R174K mutation of the PDE5-GAFa domain reduces its ability to bind cGMP *in vitro* because the substitution is located in a domain that interacts with cGMP (46) and is also predicted to alter hydrogen bonds. However, according to the *Dr*BphP crystal structure, the R384K substitution (Arg-302 in *Dr*BphP) is in an outer α-helix of the domain, more than 13 Å away from the chromophore (C ring of the open chain tetrapyrrole chromophore). A comparable conclusion (20 Å distance from the position equivalent to chromophore attachment site) can be reached by using homology modeling taking the crystal structure of the GAF domain of YKG9 (Protein Data Bank 1F5M) as template (46). Therefore, no direct interaction of the mutated site with the chromophore seems likely. The position equivalent to phyA Arg-384 in *Dr*BphP (Arg-302) forms hydrogen bonds with both Lys-297 (phyA Val-379) and Glu-127 (phyA Glu-183). Modeling the introduction of the Arg to Lys mutation disrupts the interaction between the guanidinium group of Arg-302 and the oxygen carbonyl of Lys-297. Modeling to other rotamers of Lys without moving the backbone restores both hydrogen bonds through the single N atom present in the side chain of Lys. However, a weakening of these interactions by the Arg to Lys mutation would lead to a looser structure of the protein that could account for the long distance-reaching effects.

Three additional GAF domain mutants obtained in genetic screenings have been reported, but none has been characterized *in vitro*. The $phyA^{eid4}$ allele (E229K) is hypersensitive to FR and shows normal PHYA protein levels and phyA spectral activity (47). The *phyA-110* mutant (R279S) retains WT protein levels and has been proposed to produce a P_{fr} intermediate unable to form the P_r state (48). The *phyA-109* mutant (G367S), which is the closest to *phyA-303* so far reported, shows poor responses to FR and significantly reduced levels of spectrally active phyA (48). The PHYA domain containing *phyA-303* and *phyA-109* appears to be important for protein synthesis and/or stability. Actually, the *phyA-303* mutation also caused poor protein yield in the two heterologous systems tested here (data not shown). Poor protein yield in bacteria was also observed for the W366F mutated phyA (45).

Previous reports had demonstrated the physiological activity of N-terminal domain fusions of phyB to GFP, GUS, and NLS (21, 22). The present report extends this conclusion to phyA, but some differences must be noted. First, the N-terminal phyB constructions failed to induce de-etiolation responses (short hypocotyls, open cotyledons) in dark-grown seedlings, despite the constitutive nuclear localization of these fusions. Here we observed that increasing abundance of PHYA-65-WT or PHYA-65-R384K in independent transgenic lines caused a gradual reduction in hypocotyl elongation in dark-grown seedlings (Fig. 6*C*). *A priori*, this observation admits two possible explanations. One is based on a constitutive activity of PHYA-65-WT or PHYA-65-R384K independent of the light signal, *i.e.* independently of the P_r or the P_{fr} form. In the case of cryptochromes, the C-terminal domain is able to trigger de-etiolation in darkness (49). The second explanation is based on the light stability of the PHYA-65-WT or PHYA-65-R384K fusions (Fig. 6). Full-length phyA undergoes proteolytic degradation in the P_{fr} form, a process mediated by the 26S proteasome that requires domains close to the C terminus (50). Therefore, the stability of PHYA-65-WT and PHYA-65-R384K, which lack the entire C-terminal domain, is not surprising. Light exposure during the induction of seed germination could transform seed P_r to stable P_{fr}, and the latter in turn might induce hypocotyl growth inhibition and cotyledon unfolding. Several observations favor the second interpretation. If the red light treatment given to the seeds to induce germination is terminated with a long wavelength pulse of FR to revert most of the PHYA-65 fusion protein from the P_{fr} to the P_r form, the phenotype observed in the seedlings subsequently developed in darkness is significantly reduced. In addition, at equal protein levels, the phenotype observed in dark-grown seedling was weaker for the lines bearing the mutated PHYA-65-R384K than for those bearing the PHYA-65-WT fusion. This difference could be due to the reduced ability to incorporate the chromophore caused by the R384K mutation and the requirement of photo-conversion rather than an effect of the P_r form. Finally, we had previously observed that in the WT irradiation protocols that cause seed exposure to light perceived by phyA and/or phyB in the hours immediately prior to germination (radicle protrusion) cause inhibition of hypocotyl extension in dark-grown seedlings (51). In the transgenics bearing PHYA-65-WT or PHYA-65-R384K fusions, the need for prolonged or delayed seed irradiation observed in the WT could be circumvented by the presence of a stable pool of N-terminal phyA.

Acknowledgments—We thank Dr. Richard Vierstra (University of Wisconsin) and Dr. Lee Pratt (University of Georgia, Athens) for their kind provision of monoclonal antibodies and Arabidopsis Biological Resource Center (Ohio State University) for samples of hy1 and hy2 seeds. We are indebted to Gul Koç for help with the PCB and biliverdin preparations and to Helene Steffen for help with the protein expression experiments.

REFERENCES

1. Casal, J. J., Fankhauser, C., Coupland, G., and Blázquez, M. A. (2004) *Trends Plant Sci.* **9,** 309–314
2. Chen, M., Chory, J., and Fankhauser, C. (2004) *Annu. Rev. Genet.* **38,** 87–117
3. Gärtner, W., and Braslavsky, S. E. (2004) in *Photoreceptors and Light Signaling* (Batschauer, A., ed) Vol. 3, pp. 136–180, Royal Society of Chemistry, Cambridge, UK
4. Rockwell, N. C., and Lagarias, J. C. (2006) *Plant Cell* **18,** 4–14
5. Clack, T., Mathews, S., and Sharrock, R. A. (1994) *Plant Mol. Biol.* **25,** 413–427
6. Botto, J. F., Sánchez, R. A., Whitelam, G. C., and Casal, J. J. (l996) *Plant Physiol.* **110,** 439–444

7. Shinomura, T., Nagatani, A., Hanzawa, H., Kubota, M., Watanabe, M., and Furuya, M. (1996) *Proc. Natl. Acad. Sci. U. S. A.* **93,** 8129–8133
8. Yanovsky, M. J., Casal, J. J., and Whitelam, G. C. (1995) *Plant Cell Environ.* **18,** 788–794
9. Schäfer, E., and Nagy, F. (2006) *Photomorphogenesis in Plants and Bacteria: Function and Signal Transduction Mechanisms*, Springer, Dordrecht, The Netherlands
10. Casal, J. J., Yanovsky, M. J., and Luppi, J. P. (2000) *Photochem. Photobiol.* **71,** 481–486
11. Cerdán, P. D., Staneloni, R. J., Ortega, J., Bunge, M. M., Rodríguez-Batiller, J., Sánchez, R. A., and Casal, J. J. (2000) *Plant Cell* **12,** 1203–1211
12. Yanovsky, M. J., Luppi, J. P., Kirchbauer, D., Ogorodnikova, O. B., Sineshchekov, V. A., Adam, E., Kircher, S., Staneloni, R. J., Schäfer, E., Nagy, F., and Casal, J. J. (2002) *Plant Cell* **14,** 1591–1603
13. Lagarias, J. C., and Rapoport, H. (1980) *J. Am. Chem. Soc.* **102,** 4821–4828
14. Wagner, D., Fairchild, C. D., Kuhn, R. M., and Quail, P. H. (1996) *Proc. Natl. Acad. Sci. U. S. A.* **93,** 4011–4015
15. Yeh, K.-C., and Lagarias, J. C. (1998) *Proc. Natl. Acad. Sci. U. S. A.* **95,** 13976–13981
16. Fankhauser, C., Yeh, K. C., Lagarias, J. C., Zhang, H., Elich, T. D., and Chory, J. (1999) *Science* **284,** 1539–1541
17. Quail, P. H., Boylan, M. T., Parks, B. M., Short, T. W., Xu, Y., and Wagner, D. (1995) *Science* **268,** 675–680
18. Edgerton, M. D., and Jones, A. M. (1992) *Plant Cell* **4,** 161–171
19. Cherry, J. R., Hondred, D., Walker, J. M., Keller, J. M., Hershey, H. P., and Vierstra, R. D. (1993) *Plant Cell* **5,** 565–575
20. Kircher, S., Kozma-Bognar, L., Kim, L., Adam, E., Harter, K., Schäfer, E., and Nagy, F. (1999) *Plant Cell* **11,** 1445–1456
21. Matsushita, T., Mochizuki, N., and Nagatani, A. (2003) *Nature* **424,** 571–574
22. Oka, Y., Matsushita, T., Mochizuki, N., Suzuki, T., Tokutomi, S., and Nagatani, A. (2004) *Plant Cell* **16,** 2104–2116
23. Wagner, J. R., Brunzelle, J. S., Forest, K. T., and Vierstra, R. D. (2005) *Nature* **438,** 325–331
24. Nagatani, A., Reed, J. W., and Chory, J. (1993) *Plant Physiol.* **102,** 269–277
25. Reed, J. W., Nagatani, A., Elich, T. D., Fagan, M., and Chory, J. (1994) *Plant Physiol.* **104,** 1139–1149
26. Koornneef, M., Rolf, E., and Spruit, C. J. P. (1980) *Z. Pflanzenphysiol.* **100,** 147–160
27. Davis, S. J., Kurepa, J., and Vierstra, R. D. (1999) *Proc. Natl. Acad. Sci. U. S. A.* **96,** 6541–6546
28. Kohchi, T., Mukougawa, K., Frankenberg, N., Masuda, M., Yokota, A., and Lagarias, J. C. (2001) *Plant Cell* **13,** 425–436
29. Martínez-García, J. F., Monte, E., and Quail, P. H. (1999) *Plant J.* **20,** 251–257
30. Ruddat, A., Schmidt, P., Gatz, C., Braslavsky, S. E., Gärtner, W., and Schaffner, K. (1997) *Biochemistry* **36,** 103–111
31. Hisada, A., Hanzawa, H., Weller, J., Nagatani, A., Reid, J., and Furuya, M. (2000) *Plant Cell* **12,** 1063–1078
32. Kufer, W., and Sheer, H. (1979) *Hoppe Seyler's Z. Physiol. Chem.* **360,** 935–956
33. Mc Donagh, A. F., and Palma, L. A. (1980) *Biochem. J.* **189,** 193–208
34. Clough, S. J., and Bent, A. F. (1998) *Plant J.* **16,** 735–743
35. Parks, B. M., and Quail, P. H. (1991) *Plant Cell* **3,** 1177–1186
36. Choi, G., Yi, H., Lee, J., Kwon, Y.-K., Soh, M. S., Shin, B., Luka, Z., Hahn, T.-R., and Song, P.-S. (1999) *Nature* **401,** 610–613
37. Maloof, J., Borevitz, J., Dabi, T., Lutes, J., Nehring, R., Redfern, J., Trainer, G., Wilson, J., Asami, T., Berry, C., Weigel, D., and Chory, J. (2001) *Nat. Genet.* **29,** 441–446
38. Ryu, J., Kim, J., Kunkel, T., Kim, B., Cho, D., Hong, S., Kim, S., Fernández, A., Kim, Y., Alonso, J., Ecker, J., Nagy, F., Lim, P., Song, P., Schäfer, E., and Nam, H. (2005) *Cell* **120,** 395–406
39. Schmidt, P., Gensch, T., Remberg, A., Gärtner, W., Braslavsky, S. E., and Schaffner, K. (1998) *Photochem. Photobiol.* **65,** 754–761
40. Li, L., and Lagarias, J. C. (1992) *J. Biol. Chem.* **267,** 19204–19210
41. Henning, L., Buche, C., and Schäfer, E. (2000) *Plant Cell Environ.* **23,** 727–734
42. Elich, T. D., Mc Donagh, A. F., Palma, L. A., and Lagarias, J. C. (1989) *J. Biol. Chem.* **264,** 12902–12908
43. Wu, S. H., and Lagarias, J. C. (2000) *Biochemistry* **39,** 13487–13495
44. Deforce, L., Furuya, M., and Song, P.-S. (1993) *Biochemistry* **32,** 14165–14172
45. Remberg, A., Schmidt, P., Braslavsky, S. E., Gärtner, W., and Schaffner, K. (1999) *Eur. J. Biochem.* **266,** 201–208
46. Ho, Y. S., Burden, L. M., and Hurley, J. H. (2000) *EMBO J.* **20,** 5288–5299
47. Dieterle, M., Bauer, D., Buche, C., Krenz, M., Schäfer, E., and Kretsch, T. (2005) *Plant J.* **41,** 146–161
48. Xu, Y., Parks, B. M., Short, T. W., and Quail, P. H. (1995) *Plant Cell* **7,** 1433–1443
49. Yang, H. Q., Wu, Y. J., Tang, R. H., Liu, D., Liu, Y., and Cashmore, A. R. (2000) *Cell* **103,** 815–827
50. Clough, R. C., Jordan-Beebe, E. T., Lohman, K. N., Marita, J. M., Walker, J. M., Gatz, C., and Vierstra, R. D. (1999) *Plant J.* **17,** 155–167
51. Alconada-Magliano, T., and Casal, J. J. (2004) *Photochem. Photobiol. Sci.* **3,** 612–616